Journal of CO2 Utilization 62 (2022) 102064

Contents lists available at ScienceDirect

Journal of CO2 Utilization

journal homepage: www.elsevier.com/locate/jcou

Tailoring the CO_2 selective adsorption properties of MOR zeolites by post functionalization

Dong-il Kwon [a,1], Muhammad Numan [a,1], Jungmin Kim [b,c], Murat Yilmaz [d], Sang-Eon Park [a], Hyotcherl Ihee [b,c,*], Changbum Jo [a,**]

[a] Department of Chemistry and Chemical Engineering, Inha University, 100 Inha-ro, Michuhol-gu, Incheon 22212, Republic of Korea
[b] Department of Chemistry and KI for the BioCentury, Korea Advanced Institute of Science and Technology (KAIST), Daejeon 34141, Republic of Korea
[c] Center for Advanced Reaction Dynamics, Institute for Basic Science (IBS), Daejeon 34141, Republic of Korea
[d] Department of Chemical Engineering, Osmaniye Korkut Ata University, Osmaniye 80000, Turkey

ARTICLE INFO

Keywords:
Adsorption
Zeolite
Functionalization
Carbon dioxide
Methane

ABSTRACT

A wide range of organic molecules covering benzene, dimethylbenzene, methoxybenzene, and dimethoxybenzene, isopropylbenzene with different molecular diameters were covalently attached to the interior micropore walls of mordenite (MOR) zeolites to enable the systematic tuning of adsorption properties. The formation of covalent bonds between internal oxygens of MOR and benzene carbon atoms were confirmed *via* Rietveld refinement. The adsorption properties of the functionalized MORs were studied using CO_2, CH_4, and N_2 adsorption isotherms under static conditions, and ideal adsorbed solution theory was used to predict MOR selectivities for CO_2 over CH_4 and N_2. The results showed that post-functionalization with organics remarkably improved CO_2/CH_4 and CO_2/N_2 selectivities, albeit at the expense of a slight concomitant partial loss of CO_2 adsorption capacity. Among the functionalized zeolites, the MOR functionalized with isopropylbenzene (the bulkiest moiety introduced) exhibited the highest selectivities ($CO_2/CH_4 = 18.3$, $CO_2/N_2 = 59.9$), which were 2.8 and 4.3 times higher, respectively, than those of pristine MOR ($CO_2/CH_4 = 6.6$, $CO_2/N_2 = 14$). Reduction of effective micropore diameters by isopropylbenzene is responsible for the improved CO_2 adsorption selectivity. We believe that the concept of tailoring the molecular-sieve properties of zeolites by organic functionalization will open new opportunities for developing efficient molecular sieves for chemical separation processes.

1. Introduction

Carbon dioxide (CO_2) emission is a primary concern when considering the compositions of greenhouse gases released into the atmosphere by industry, transport, and the energy-producing sector [1–3]. Technological research on CO_2 capture conducted during the last century reduced environmental impacts by reducing the levels of noxious flue gases before releasing them into the atmosphere. Technologies that capture CO_2 are not only useful for the purification of natural gas [4–7], but are also important in terms of converting CO_2 into useful products [8,9]. The removal of CO_2 from natural gas streams is an important topic in research and industry in the context of producing methane (CH_4) streams containing lower CO_2 levels, and efforts are underway to improve gas separation processes by devising efficient adsorbents. CO_2 removal by amine absorption is the traditional method but is no longer cost-effective due to high chemical and energy costs and the required high-temperature regeneration. The pressure swing adsorption (PSA) method is the best alternative to amine-based processes, but equilibrium adsorption information is needed to enable the selection of appropriate adsorbents for PSA. In this context, Ideal Adsorbed Solution Theory (IAST), derived from single-component isotherms, was proposed by Myers and Prausnitz [10] to predict selectivity for one gaseous

---

Abbreviations: MOR, Mordenite; *uf*-MOR, Unfunctionalized MOR; Ph, Benzene; Me2Ph, 3,5-Dimethyl phenyl; MeO2Ph, 3,5-di-methoxy phenyl; *i*PrPh, iso-propyl phenyl; MeOPh, methoxy phenyl.

* Corresponding author at: Department of Chemistry and KI for the BioCentury, Korea Advanced Institute of Science and Technology (KAIST), Daejeon 34141, Republic of Korea.

** Corresponding author.

E-mail addresses: hyotcherl.ihee@kaist.ac.kr (H. Ihee), jochangbum@inha.ac.kr (C. Jo).

[1] These authors contributed equally to this work.

https://doi.org/10.1016/j.jcou.2022.102064
Received 9 March 2022; Received in revised form 11 May 2022; Accepted 12 May 2022

component over others. This theory assumes that the adsorbed phase is equally accessible to all compounds and is a temperature-invariant field. Also, according to this theory, the adsorbed mixture for each solute forms an ideal solution in equilibrium with the bulk (gas or liquid) phase at constant diffusion pressure [10]. Adsorbent-adsorbate interactions are of central importance when determining the equilibrium selectivity for a particular gas, and these interaction forces are highly dependent on the molecular natures of adsorbates and the surface of solid adsorbents. In this regard, the surface of solid adsorbents such as carbon was post-synthetically modified to enhance the CO_2 adsorption performance. [11–13].

Crystalline microporous materials with molecular-sieving capabilities are candidate physical adsorbents [14–19], and zeolites are one of the most widely used materials owing to their low costs and thermal and hydrothermal stabilities. Zeolites are crystalline microporous aluminosilicates, in which tetrahedral SiO_4 and AlO_4 species are three-dimensionally interconnected through bridging oxygens to form porous structures with uniform micropores. Zeolites are potential candidates for CO_2 capture applications at the bench and industrial scales due to their physical properties, including high porosity, molecular scale pore dimensionality, and intrapore ion-exchange ability. Zeolites can form many different crystal structures depending on how TO_4 (T = Si or Al) units are connected, and so far, more than 200 crystal structures have been discovered [20–25]. Mordenite (MOR) is a well-known zeolite and contains unidirectional array of microporous channels along its *c* axis. The aperture of each channel is formed by a 12-oxygen ring of diameter of ~ 7 Å [26–30]. In addition, MOR has a high ion exchange capacity for metal cations due to its low Si/Al ratio [27].

Modifying porous materials by attaching differently sized organic molecules provides means of improving the molecular-sieve properties of zeolites [31]. The use of organosilane or tetraorthosilicate as grafting agents involves condensation reaction between these agents and substrate ≡Si—OH groups [32]. However, functionalization performed using this method is limited to the outer crystal surfaces of zeolites and does not affect inner micropores [33], because the molecular dimensions of organosilanes are much larger than those of zeolite pores, which prevents organosilanes from accessing micropores [31]. As a result, organic functionalization of microporous zeolites has been considered ineffective, and few studies have been conducted on post-synthetic modifications of zeolite micropores. On the other hand, a study has drawn our attention that organic moieties can be attached to zeolite micropore walls using organic diazonium derivatives as grafting agents [34]. This method of post-synthetic functionalization enabled the molecular-sieve properties of zeolites to be fine-tuned and resulted in a dramatic enhancement of ethylene selectivity over ethane. Here, we extended this concept of tailoring the molecular-sieve properties to improve the CO_2/N_2 and CO_2/CH_4 separation processes. Based on the calculation of the gyration radius for various organic molecules, five of them with different gyration radius were chosen as the grafting agents for zeolite functionalization. MOR zeolites were then functionalized with various organic groups of different molecular sizes for tuning its adsorption properties (Scheme 1), and these were studied using CO_2, CH_4, and N_2 adsorption isotherms under static conditions. MOR zeolite was chosen based on our previous report, in which a zeolite with 1-dimensional channel system (MOR, LTL) is more sensitive than 3-dimensional channel zeolites (*e.g.*, FAU), in terms of tailoring the molecular sieving effect by organic post-functionalization. Ideal adsorbed solution theory (IAST) was applied to isotherm data to obtain predicted selectivity of CO_2 over CH_4 and N_2.

2. Materials and methods

2.1. Materials

Mordenite zeolite (CBV10A, Na^+ form, SiAl = 6.5) was purchased from Zeolyst International (USA), acetone (99.5%), and benzene (99.5%) from Samchun Chemicals (South Korea), and tetrafluoroboric acid solution, ethanol, and aniline from Sigma-Aldrich (USA). 4-Methoxybenzenediazonium tetrafluoroborate was purchased from TCI (Japan). Benzene diazonium derivatives were synthesized according to a previous work [34], except that 4-methoxybenzenediazonium tetrafluoroborate was purchased from Alfa Aesar (USA).

2.2. Post-functionalization of MOR zeolites

MOR was degassed for 4 h and was immediately dispersed in 10 g of benzene. Subsequently, to this solution, 20 wt% of diazonium derivative was added. The resulting solution was stirred at room temperature for 2 h, heated to 343 K for 8 h, filtered, washed with benzene, and dried at 353 K overnight. To completely remove benzene and residual benzene diazonium derivate, samples were washed with methanol and then dried in a vacuum oven at 363 K overnight.

2.3. Characterization

N_2 adsorption/desorption isotherms at 77 K were obtained using a Micromeritics Tristar 3020 analyzer (USA). Before measurement, samples were degassed at 523 K for 4 h. The Brunauer-Emmett-Teller (BET) equation was used to calculate surface areas using an adsorption branch at a relative pressure (P/P_0) of 0.05–0.3. CO_2 and N_2 adsorption isotherms at 283 K and 293 K, respectively, were obtained using a Belsorp mini II (Japan). Thermogravimetric analysis (TGA) data were obtained using a Bruker TG-DTA2000SA instrument (USA). Elemental analysis (EA) was performed using a FlashSmart™ elemental analyzer (Thermo Scientific, USA). X-ray diffraction (XRD) patterns were obtained using a Rigaku Miniflex instrument (Japan) and a Cu Kα source (λ = 0.154 nm) at 30 kV and 15 mA.

2.4. Radius of gyration

Radii of gyration, R_g, of functional groups were calculated from atomic coordinates. As a first step to calculate R_g values, the coordinates of the center of masses of functional groups were calculated using the following Eq. (1),

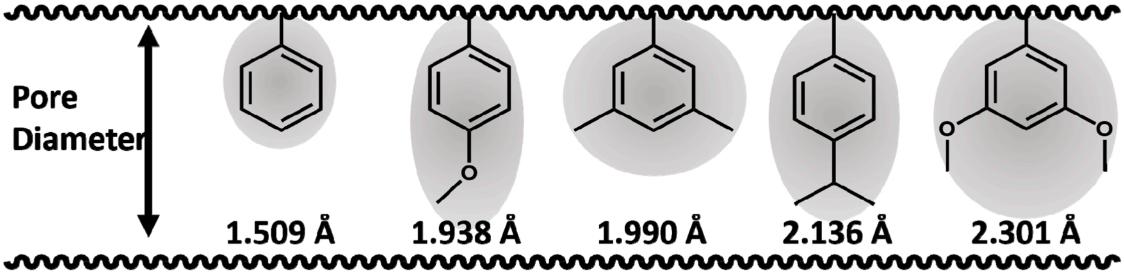

Scheme 1. Schematic illustration of tuning the effective pore size of zeolite by postsynthetic modification with various organic groups having different molecular sizes. The Arabic numeral below the organics indicates their radius of gyration.

$$x_{cm} = \frac{\sum_{i=1}^{n} m_i x_i}{\sum_{i=1}^{n} m_i}, y_{cm} = \frac{\sum_{i=1}^{n} m_i x_i}{\sum_{i=1}^{n} m_i}, z_{cm} = \frac{\sum_{i=1}^{n} m_i x_i}{\sum_{i=1}^{n} m_i} \quad (1)$$

where x_{cm}, y_{cm} and z_{cm} are the x, y and z coordinates, respectively, of the center of mass of a functional group, n is the number of atoms in the atomic coordinates, m_i is the atomic mass of the ith atom, x_i, y_i, and z_i are the x, y, and z coordinates of the ith atom, respectively. Then, R_g values were calculated using the following Eq. (2):

$$R_g = \sqrt{\frac{\sum_{i=1}^{n} m_i \quad \{(x_i - x_{cm})^2 + (y_i - y_{cm})^2 + (z_i - z_{cm})^2\}}{\sum_{i=1}^{n} m_i}} \quad (2)$$

2.5. *IAST selectivity*

Ideal CO_2 selectivities in CO_2/CH_4 and CO_2/N_2 mixtures were calculated using the pyIAST program in the Python package. To calculate selectivities, pure-component adsorption isotherm data obtained using the Belsorp mini II instrument were used. CO_2 adsorption data were fitted using the dual-site Freundlich and BET model, and N_2 and CH_4 adsorptions were fitted using the single-site Freundlich model, because of the small numbers of molecules adsorbed. [35].

3. Results and discussion

3.1. *Characterization of the organic-functionalized MOR zeolites*

MOR zeolite is composed of 12-member rings (12 MR) channels orientated in the c-direction [26]. These channels have elliptically shaped pore orifices of diameters of 6.5 and 7.0 Å (Fig. 1). Along the channel system, Na^+ cations are distributed as compensation cations to balance the negative charge of the zeolite framework, and they might be located nearby T3 and T4 sites of MOR zeolites according to the suggestion by Bodart. [34].

Commercially available MOR zeolite (CBV 10 A; denoted by *uf*_MOR) was functionalized with benzene molecules using phenyl diazonium tetrafluoroborate as the grafting agents in acetonitrile, as previously described [34,36,37]. The resulting zeolite is denoted by Ph_*f*_MOR. The powder XRD patterns of *uf*_MOR and Ph_*f*_MOR showed that no conspicuous loss of zeolite crystallinity is observed after functionalization (Fig. S1), and elemental analysis showed that Ph_*f*_MOR (Table S1) contained 1.29 wt% carbon.

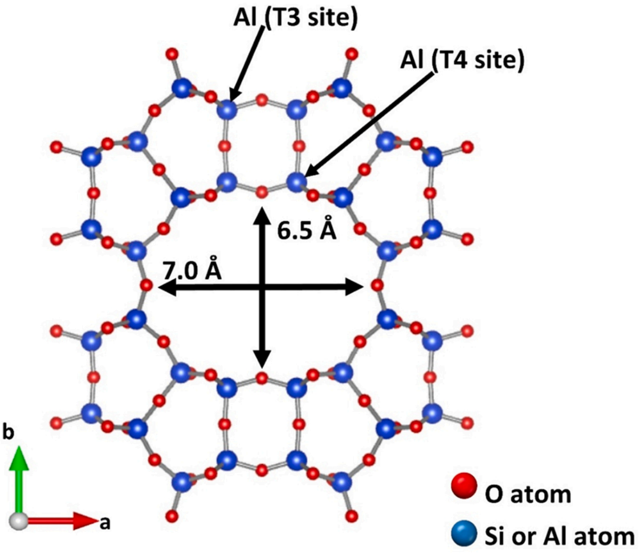

Fig. 1. MOR structure showing 12 MR channel in the plane perpendicular to the c-axis.

Covalent attachment of Ph to MOR micropores was confirmed by solving the crystal structure of Ph_*f*_MOR using synchrotron powder XRD data and Rietveld refinement (Fig. 2 and Table S2). According to the obtained structure, the length of the bond between Ph carbon and bridging oxygen of 12 MR was 1.52 Å (Fig. 2e). The paraffin C-O bond length (1.43–1.60 Å) ensured that Ph-groups were covalently bonded to 12 MR oxygens of MOR. Various organic molecules with different gyration radii were attached to MOR micropores using appropriate diazonium benzene derivatives (see Fig. S2a for their molecular structures).

This functionalization was performed based on the assumption that the grafted organic molecules might tune zeolite adsorption properties by reducing the sizes of micropores in a predictable manner. To tune the effective pore diameters in a systematically way (Scheme 1), five organic molecules having different radius of gyration were selected (Fig. S2b). To minimize the effect of chemical interaction between CO_2 and functional group, polar functional groups such as $-NH_2$, -SH, -OH and -COOH were excluded. The functionalized MOR produced are denoted by X_*f*_MOR, where X is the functionalizing entity, *e.g.*, 4-methoxybenzene [MeOPh], di-methyl benzene [$(Me)_2$Ph], di-methoxy benzene [$(MeO)_2$Ph], or isopropyl benzene [*i*PrPh].

The N_2 adsorption-desorption isotherms of *uf*_MOR and X_*f*_MORs showed that after functionalization, N_2 adsorption into zeolite micropores was negligible (Fig. S3). The surface areas of *uf*_MOR, Ph_*f*_MOR, $(Me)_2$Ph_*f*_MOR, MeOPh_*f*_MOR, $(MeO)_2$Ph_*f*_MOR, and *i*PrPh_*f*_MOR were 468, 32.2, 17.4, 12.9, 14.7, and 24.3 m^2 g^{-1}, respectively. The surface areas of functionalized MORs are significantly smaller than that of *uf*_MOR, indicating their micropore diameters were severely reduced, which limited N_2-adsorption at cryogenic temperatures [31]. The carbon contents of functionalized MORs are provided in Table S1. In addition, TGA curve for Ph_*f*_MOR shows the first detectable weight loss at 450 K and a second one at 750 K. The former loss weight loss is associated with the desorption of water and the latter one is attributed to the decomposition of organic molecules. The weight loss at such high temperature confirms the presence of strongly linked organic reagents in the zeolite framework (Fig. S4).

3.2. *Gas adsorption properties of functionalized zeolites*

Five functionalized MORs, that is, Ph_*f*_MOR, $(Me)_2$Ph_*f*_MOR, MeOPh_*f*_MOR, $(MeO)_2$Ph_*f*_MOR, and *i*PrPh_*f*_MOR, were prepared and sorption isotherms were obtained at 288 K and 298 K to investigate the effect of functionalization and consider potential applications in terms of CH_4, CO_2, and N_2 adsorption (Fig. 3). To show the difference in gas adsorption more clearly, the expanded image of CH_4, CO_2, and N_2 isotherms for functionalized MORs are displayed in Fig. S5. For all functionalized MORs, adsorption increased with increase in pressure and decreased with increase in temperature (at 298 K *vs.* 288 K) for CO_2, CH_4, and N_2.

CH_4 adsorptions of functionalized MORs were examined at 288 K and 298 K (Fig. 3a and b). Adsorption capacities were from 0.88 to 0.98 mmol g^{-1} at 288 K and 0.59–0.62 mmol g^{-1} at 298 K, except for MeOPh_*f*_MOR, which had a higher capacity of 0.74 mmol g^{-1} at 298 K. The order of CH_4 adsorption at 288 K was; Ph_*f*_MOR > $(Me)_2$Ph_*f*_MOR > $(MeO)_2$Ph_*f*_MOR ≈ *i*PrPh_*f*_MOR > MeOPh_*f*_MOR. N_2 adsorption capacities of Ph_*f*_MOR, $(Me)_2$Ph_*f*_MOR, MeOPh_*f*_MOR, $(MeO)_2$Ph_*f*_MOR, and *i*PrPh_*f*_MOR for the same adsorbents varied between 0.32 and 0.49 mmol g^{-1} at 288 K and 0.28–0.4 mmol g^{-1} at 298 K (Fig. 3c and d). N_2 adsorptions at 288 K followed the same order as those for CH_4, though adsorption capacities were slightly lower, which we believe were due to the different polarizabilities of N_2 and CH_4 (17.4×10^{25} cm^3 *vs.* 25.9×10^{25} cm^3) [33].

CO_2 adsorption isotherm of the five functionalized adsorbents were obtained under the same experimental conditions used for CH_4 and N_2

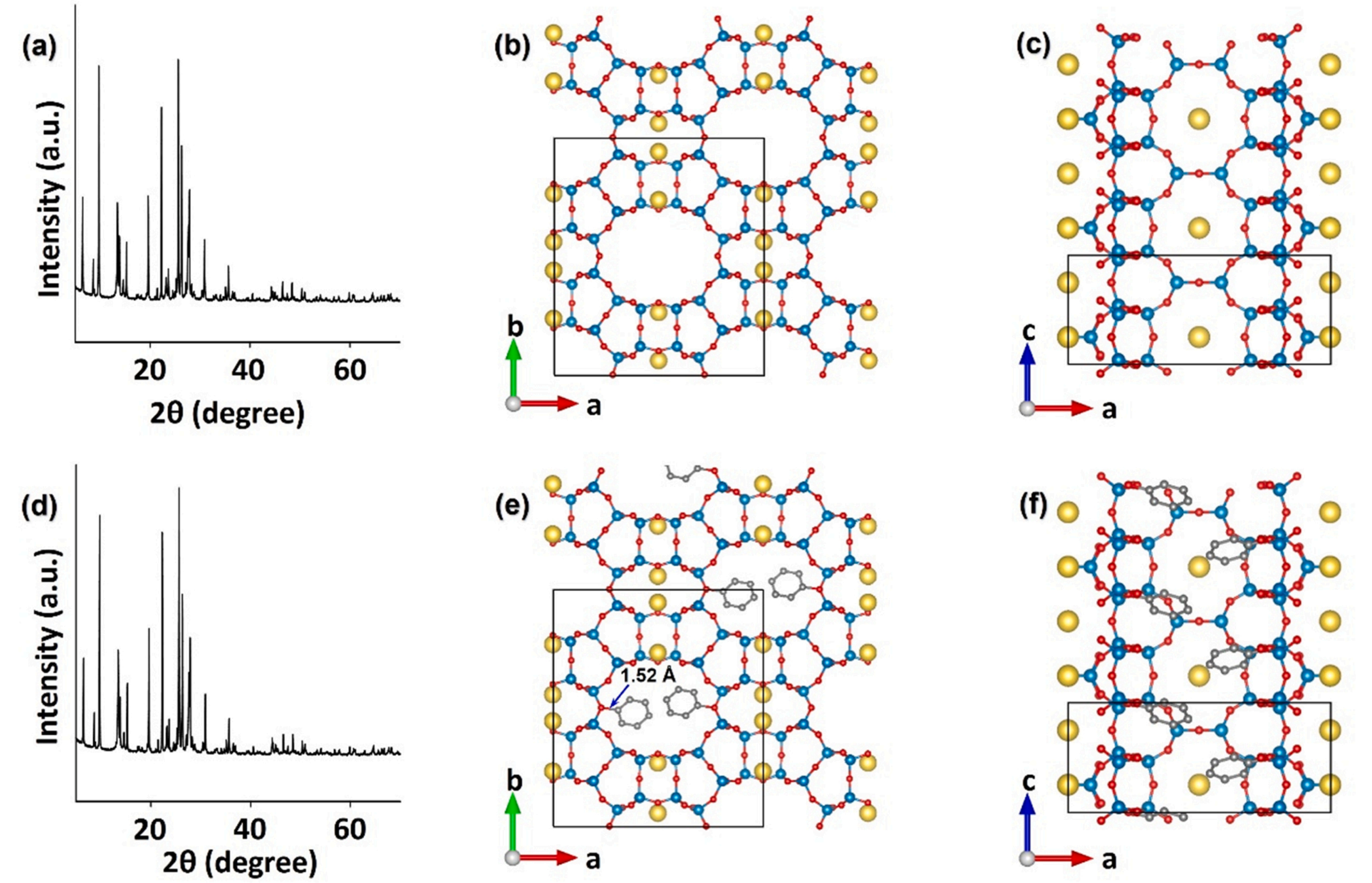

Fig. 2. Synchrotron powder X-ray diffraction patterns for (a) *uf*_MOR and (d) Ph_*f*_MOR and the corresponding crystal structures obtained by Rietveld refinement on (b, c) *uf*_MOR and (e, f) Ph_*f*_MOR.

(Fig. 3e and f). *uf*_MOR had CO_2 adsorption capacities of 3.3 and 3.2 mmol g^{-1} at 288 K and 298 K and Ph_*f*_MOR had values of 2.1 and 1.9 mmol g^{-1}, respectively. The CO_2 adsorption capacities of the other functionalized adsorbents varied from 2.1 to 2.2 mmol g^{-1} at 288 K and 1.8–2.1 mmol g^{-1} at 298 K. When CO_2 isotherms were compared with N_2 and CH_4 isotherms, CO_2 adsorption capacities were greater than those of CH_4 and N_2 presumably because CO_2 molecules are linear and have a smaller kinetic diameter and higher critical temperature (304.12 K) than CH_4 (190.56 K)/ N_2 (126.2 K). Furthermore, CO_2 has a high polarizability and a quadrupole moment as well.

3.3. Ideal adsorption solution theory (IAST) selectivity of CO_2 over CH_4 and N_2

IAST selectivities of CO_2 over CH_4 and N_2 were derived from the N_2, CH_4, and CO_2 static isotherms. Fig. 4a shows the calculated CO_2 selectivities of *uf*_MOR and *f*_MOR at 298 K for a gas mixture containing 15 vol% CH_4 and 85 vol% N_2 from 0 to 101 kPa. All *f*_MOR samples exhibited higher CO_2 selectivity compared to *uf*_MOR. Specifically, the order of CO_2 selectivities at 10 kPa for the functionalized MORs and *uf*_MOR was; *i*PrPh_*f*_MOR (18.3) > (Me)$_2$Ph_*f*_MOR (17.4) > (MeO)$_2$Ph_*f*_MOR (13.4) > MeOPh_*f*_MOR (12.7) > Ph_*f*_MOR (12.6) > *uf*_MOR (6.6). Furthermore, CO_2 IAST selectivities gradually increased with increase in pressure (Fig. 4a).

In the case of IAST selectivities of CO_2 over N_2 at 10 kPa, *i*PrPh_*f*_MOR also exhibited the highest IAST selectivity of 59.9, and decreased in the order of (Me)$_2$Ph_*f*_MOR (55.4) > (MeO)$_2$Ph_*f*_MOR (47.2) > Ph_*f*_MOR (41.3) > MeOPh_*f*_MOR (36.9) > *uf*_MOR (14) (Fig. 4b). Similarly, CO_2/N_2 selectivities increased with the total pressure. This result indicates that the partial blocking of MOR micropores by organic molecules enhanced the CO_2/CH_4 and CO_2/N_2 separation performance and the degree of improvement is likely relevant to the size of functionalized organic molecules. That is, the attachment of bulky organics is more effective for enhancing the selective adsorption of CO_2 over CH_4 and N_2. The CO_2/CH_4 and CO_2/N_2 selectivity value of functionalized MOR samples prepared in this work was compared with the previously reported adsorbents in Table S4.

4. Conclusions

The inner channels of MOR zeolites were successfully functionalized with organic molecules of various sizes using diazonium derivatives. The introduction of organic molecules into zeolite micropores enhanced separation performance for gas molecules with sizes closer or similar to the pore sizes altered by functionalization. This approach enabled the adsorption properties of commercial MOR zeolites to be predictably tuned. CO_2, CH_4, and N_2 adsorption isotherms were examined at 288 K and 298 K. Compared with pristine MOR, functionalized MORs adsorbed smaller amounts of CO_2, N_2 and CH_4. On increasing the temperature to 298 K from 288 K, adsorptions decreased because the equilibrium shifted toward desorption. Calculated IAST selectivity was successfully applied to simulate adsorption equilibria for *uf*_MOR and *f*_MOR in CO_2/CH_4 and CO_2/N_2 mixtures. The highest CO_2 selectivity for CO_2/CH_4 mixture was observed for *i*PrPh_*f*_MOR (18.3), while that for CO_2/N_2 mixtures was highest for *i*PrPh_*f*_MOR (59.9), which was about 4.3 times greater than that of pristine MOR. These observations show that functionalization with organic molecules having larger radii of gyration restricts the diffusion of gas molecules into zeolite micropores. In addition to the change in size of pore aperture, a wide range of organic functional groups can be covalently attached onto the micropore walls to tailor the

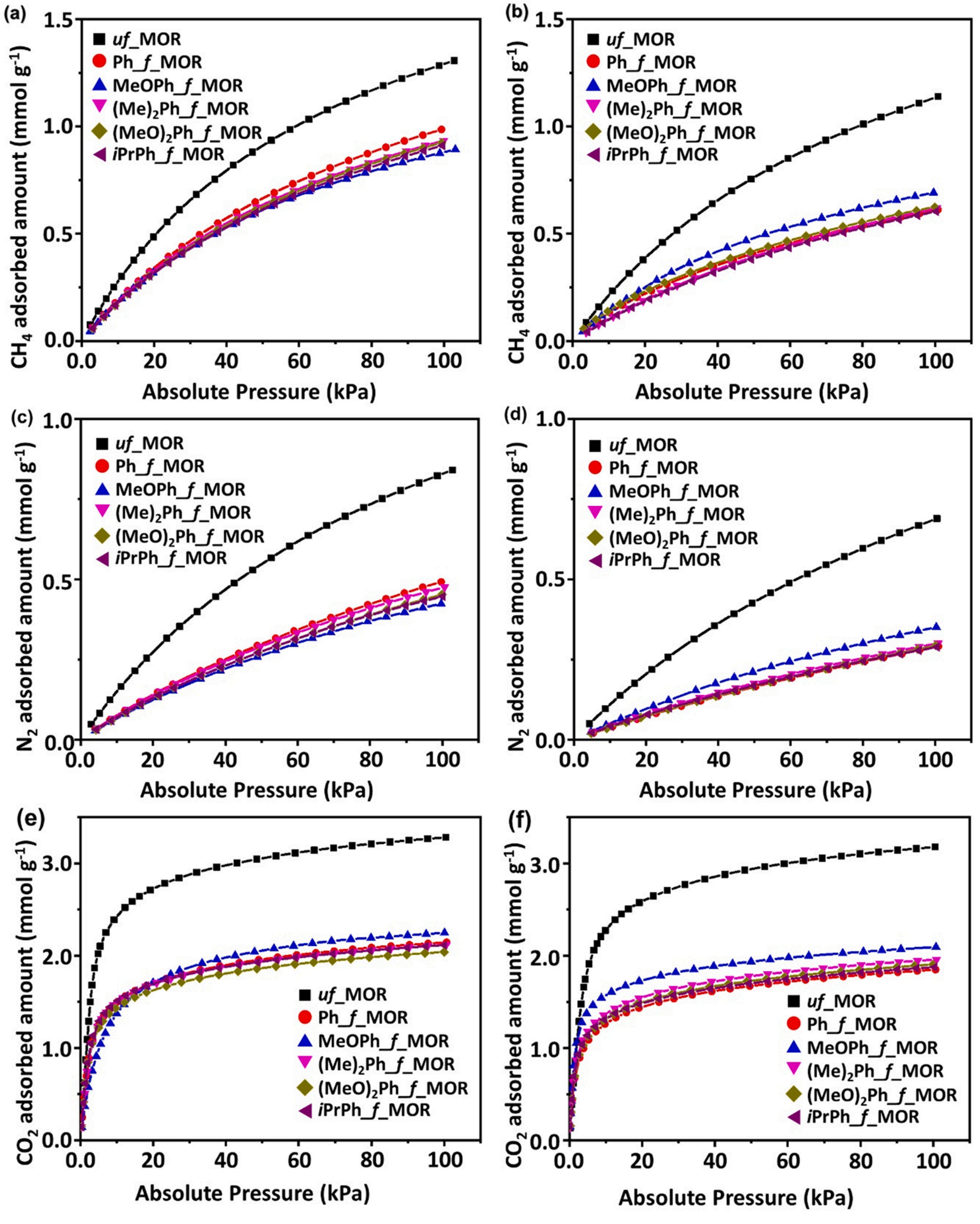

Fig. 3. Adsorption isotherms of CH_4 (a-288 K, b-298 K), N_2 (c-288 K, d-298 K), and CO_2 (e-288 K, f-298 K) on *uf*_MOR, Ph_*f*_MOR, MeOPh_*f*_MOR, *i*PrPh_*f*_MOR, $(Me)_2$Ph_*f*_MOR, and $(MeO)_2$Ph_*f*_MOR.

surface properties. Through the synergistic effect between molecular sieves and organic functional groups, the described concept provides means of producing zeolite adsorbents that selectively adsorb targeted gas molecules.

Funding sources

This work was supported by "Carbon Upcycling Project for Platform Chemicals'' (Project No. 2022M3J3A1046017) through the National Research Foundation (NRF) funded by the Ministry of Science and ICT, Republic of Korea. This work was supported by Institute for Basic Science (IBS-R033).

Associated content supporting information

EA for functionalized MOR zeolite; Atomic parameters; XRD; Gyration radii; N_2 isotherms; TGA.

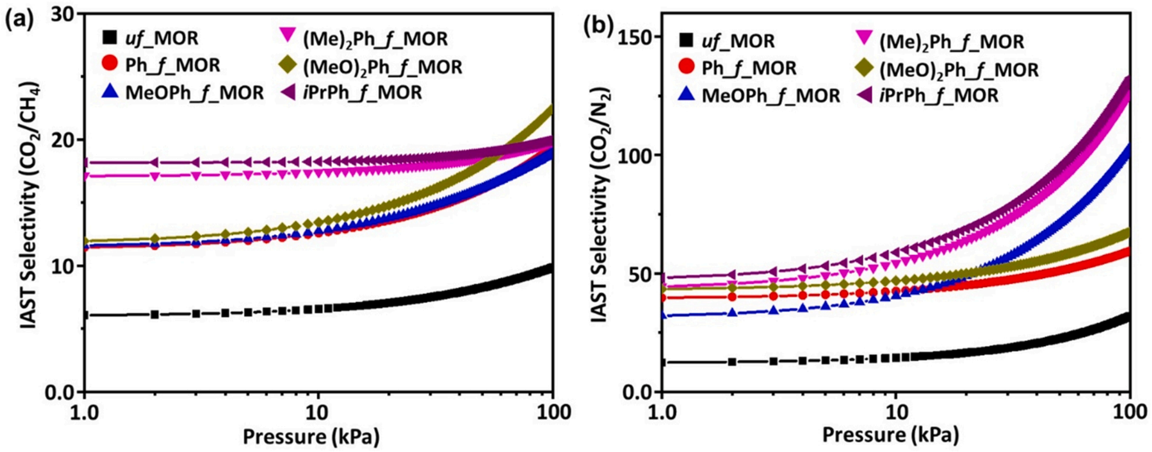

Fig. 4. Calculated IAST selectivities of CO_2 over CH_4 (a) and N_2 (b) at 298 K for gas mixture containing 15 vol% CO_2 and 85 vol% N_2 from 0 to 100 kPa for *uf*_MOR, Ph_*f*_MOR, MeOPh_*f*_MOR, *i*PrPh_*f*_MOR, (Me)$_2$Ph_*f*_MOR, and (MeO)$_2$Ph_*f*_MOR.

CRediT authorship contribution statement

Dong-il Kwon: Formal analysis, Theoretical Calculation (IAST), Review, Visualization **Muhammad Numan**: Writing – original draft, Visualization, Data curation **Jungmin Kim**: Theoretical calculations **Murat Yilmaz**: Writing **Sang-Eon Park**: Supervision **Hyotcherl Ihee**: Theoretical Calculations, Writing – review & editing **Changbum Jo**: Conceptualization, Writing – review & editing, Supervision.

Declaration of Competing Interest

The authors declare that they have no known competing financial interests or personal relationships that could have appeared to influence the work reported in this paper.

Acknowledgment

This work was supported by the National Research Foundation of Korea (NRF) grants funded by the Korea government (MSIT) (Project No. 2019M1A2A6071804). This work was supported by Institute for Basic Science (IBS-R033).

Appendix A. Supporting information

Supplementary data associated with this article can be found in the online version at doi:10.1016/j.jcou.2022.102064.

References

[1] G. Delahay, B. C, Zeolites for Cleaner Technologies, Imperial College Press, London, 2002, p. 345.
[2] S. Kumar, R. Srivastava, J. Koh, Utilization of zeolites as CO_2 capturing agents: advances and future perspectives, J. CO2 Util. 41 (2020), 101251.
[3] M. Karimi, M. Shirzad, J.A. Silva, A.E. Rodrigues, Biomass/biochar carbon materials for CO_2 capture and sequestration by cyclic adsorption processes: A review and prospects for future directions, J. CO2 Util. 57 (2022), 101890.
[4] W.A. Rizal, S.K. Wahono, Biogas filter based on local natural zeolite materials, Int. J. Renew. Energy Dev. 3 (2014) 1–5.
[5] E.L. First, M.M.F. Hasan, C.A. Floudas, Discovery of novel zeolites for natural gas purification through combined material screening and process optimization, AIChE J. 60 (2014) 1767–1786.
[6] Y. Liu, J. Hou, Selective adsorption of CO_2/CH_4 mixture on clay-rich shale using molecular simulations, J. CO2 Util. 39 (2020), 101143.
[7] J. Park, S.Y. Cho, M. Jung, K. Lee, Y.C. Nah, N.F. Attia, H. Oh, Efficient synthetic approach for nanoporous adsorbents capable of pre- and post-combustion CO_2 capture and selective gas separation, J. CO2 Util. 45 (2021), 101404.
[8] S.Y. Pan, A. Chang, Y.P. Lin, H. Kim, P.C. Chiang, An innovative approach to integrated carbon mineralization and waste utilization: a review, Aerosol Air Qual. Res. 15 (2015) 1072–1091.
[9] P. Li, S.Y. Pan, S. Pei, Y.J. Lin, P.C. Chiang, Challenges and perspectives on carbon fixation and utilization technologies: an overview, Aerosol Air Qual. Res. 16 (2016) 1327–1344.
[10] A.L. Myers, J.M. Prausnitz, Thermodynamics of mixed-gas adsorption, AIChE J. 11 (1965) 121–127.
[11] U. Kamran, S.-J. Park, Tuning ratios of KOH and NaOH on acetic acid-mediated chitosan-based porous carbons for improving their textural features and CO_2 uptakes, J. CO2 Util. 40 (2020), 101212.
[12] U. Kamran, S.-J. Park, Chemically modified carbonaceous adsorbents for enhanced CO_2 capture: a review, J. Clean. Prod. 290 (2021), 125776.
[13] U. Kamran, J.R. Choi, S.-J. Park, A role of activators for efficient CO_2 affinity on polyacrylonitrile-based porous carbon materials, Front. Chem. (2020) 710.
[14] T. Kim, B. Paul, D. Kwon, S. Nam, C. Jo, Nickel nanoparticles supported on nonreducible mesoporous materials: effects of framework types on the catalytic decomposition of methane, Bull. Korean Chem. Soc. 42 (2021), 186-171.
[15] F. Akhtar, Q. Liu, N. Hedin, L. Bergström, Strong and binder free structured zeolite sorbents with very high CO_2-over-N_2 selectivities and high capacities to adsorb CO_2 rapidly, Energy Environ. Sci. 5 (2012) 7664–7673.
[16] M. Oschatz, M. Antonietti, A search for selectivity to enable CO_2 capture with porous adsorbents, Energy Environ. Sci. 11 (2018) 57–70.
[17] A.S. Jalilov, Y. Li, C. Kittrell, J.M. Tour, Increased CO_2 selectivity of asphalt-derived porous carbon through introduction of water into pore space, Nat. Energy 2 (2017) 932–938.
[18] W. Xu, J. Wang, F. Ding, X. Chen, E. Nasybulin, Y. Zhang, J.G. Zhang, Lithium metal anodes for rechargeable batteries, Energy Environ. Sci. 7 (2014) 513–537.
[19] H. Guo, J.B. Callaway, J.P. Ting, Inflammasomes: mechanism of action, role in disease, and therapeutics, Nat. Med. 21 (2015) 677–687.
[20] Z. Bao, L. Yu, Q. Ren, X. Lu, S. Deng, Adsorption of CO_2 and CH_4 on a magnesium-based metal organic framework, J. Colloid Interface Sci. 353 (2011) 549–556.
[21] Y. Chen, B. Wang, L. Zhao, P. Dutta, W.W. Ho, New Pebax®/zeolite Y composite membranes for CO_2 capture from flue gas, J. Membr. Sci. 495 (2015) 415–423.
[22] T.S. Frantz, W.A. Ruiz, C.A. da Rosa, V.B. Mortola, Synthesis of ZSM-5 with high sodium content for CO_2 adsorption, Microporous Mesoporous Mater. 222 (2016) 209–217.
[23] N. Hedin, L. Andersson, L. Bergström, J. Yan, Adsorbents for the post-combustion capture of CO_2 using rapid temperature swing or vacuum swing adsorption, Appl. Energy 104 (2013) 418–433.
[24] R. Hernández-Huesca, L. Díaz, G. Aguilar-Armenta, Adsorption equilibria and kinetics of CO_2, CH_4 and N_2 in natural zeolites, Sep. Purif. Technol. 15 (1993) 163–173.
[25] R. Krishna, J.M. van Baten, In silico screening of zeolite membranes for CO_2 capture, J. Membr. Sci. 360 (2010) 323–333.
[26] K.M. Konysheva, T.M. Boichuk, O.V. Shvets, Effect of structural, size, and acid characteristics of hierarchical BEA and MOR zeolites on their activity in the catalytic reduction of N_2O and no by propylene, Theor. Exp. Chem. 52 (2016) 90–96.
[27] S. Jeong, K.J. Jeon, Y.K. Park, B.J. Kim, K.H. Chung, S.C. Jung, Catalytic properties of microporous zeolite catalysts in synthesis of isosorbide from sorbitol by dehydration, Catalysts 10 (2020) 148.
[28] B. Bensafi, N. Chouat, F. Djafri, High performance of carbon dioxide adsorption of mesoporous mordenite synthesized in the presence of N, N-dimethylaniline, Res. Chem. Intermed. 43 (2017) 7443–7456.
[29] T. Puspitasari, M. Ilmi, N. Nurdini, R.R. Mukti, C.L. Radiman, D. Darwis, G.T. M. Kadja, The physicochemical characteristics of natural zeolites governing the adsorption of Pb^{2+} from aqueous environment, Key Eng. Mater. 811 (2019) 92–98.
[30] H.I. Hamoud, V. Valtchev, M. Daturi, Selective catalytic reduction of NO_x over Cu- and Fe-exchanged zeolites and their mechanical mixture, Appl. Catal. B. 250 (2019) 419–428.

[31] V. Valtchev, G. Majano, S. Mintova, J. Pérez-Ramírez, Tailored crystalline microporous materials by post-synthesis modification, Chem. Soc. Rev. 42 (2013) 263–290.

[32] S.J. Reitmeier, O.C. Gobin, A. Jentys, J.A. Lercher, Enhancement of sorption processes in the zeolite H-ZSM5 by postsynthetic surface modification, Angew. Chem. Int. Ed. 48 (2008) 533–538.

[33] A. Cauvel, D. Brunel, F. Di Renzo, P. Moreau, F. Fajula, Functionalization of Y zeolites with organosilane reagents, Stud. Surf. Sci. Catal. 94 (1995) 286–293.

[34] H.S. Lee, N.S. Kim, D.I. Kwon, S.K. Lee, M. Numan, T. Jung, K. Cho, M. Mazur, H. S. Cho, C. Jo, Post-synthesis functionalization enables fine-tuning the molecular-sieving properties of zeolites for light olefin/paraffin separations, Adv. Mater. 33 (2021), 2105398.

[35] C.M. Simon, B. Smit, M. Haranczyk, pyIAST: Ideal adsorbed solution theory (IAST) Python package, Comput. Phys. Commun. 200 (2016) 364–380.

[36] K.M. Lee, N.S. Kim, M. Numan, J.C. Kim, H.S. Cho, K. Cho, C. Jo, Postsynthetic modification of zeolite internal surface for sustainable capture of volatile organic compounds under humid conditions, ACS Appl. Mater. Interfaces 13 (2021) 53925–53934.

[37] D. Kwon, J.C. Kim, H. Lee, W. Lee, C. Jo, Engineering micropore walls of beta zeolites by post-functionalization for CO_2 adsorption performance screening under humid conditions, Chem. Eng. J. 427 (2022), 131461.